JTTEE5 13:377-380
DOI: 10.1361/10599630420407
1059-9630/$19.00 © ASM International

Fracture Mechanics Analysis of Microcracks in Thermally Cycled Thermal Barrier Coatings

Y. Liu, C. Persson, and S. Melin

(Submitted September 2, 2003; in revised form November 20, 2003)

The effects from thermal shock loading on pre-existing microcracks within thermal barrier coatings (TBCs) have been investigated through a finite element based fracture mechanical analysis. The TBC system consists of a metallic bond coat and a ceramic top coat. The rough interface between the top and bond coats holds an alumina oxide layer. Stress concentrations at the interface due to the interface roughness, as well as the effect of residual stresses, were accounted for. At the eventual closure between the crack surfaces, Coulomb friction was assumed. To judge the risk of fracture from edge cracks and centrally placed cracks, the stress intensity factors were continuously monitored during the simulation of thermal shock loading of the TBC. It was found that fracture from edge cracks is more likely than from centrally placed cracks. It was also concluded that the propagation of an edge crack is already initiated during the first load cycle, whereas the crack tip position of a central crack determines whether propagation will occur.

Keywords: central crack, edge crack, finite element method, thermal barrier coatings

1. Introduction

Conventional plasma-sprayed thermal barrier coatings (TBCs), consisting of an yttria partially stabilized zirconia ceramic top coat and a metallic bond coat, are frequently used to protect hot-section components in gas turbines to enhance the performance and to increase the component life. The failure of such TBCs is often reported to occur through delamination as a result of in-plane cracking in the top coat adjacent to the ceramic/metal interface during cyclic thermal exposure. The presence of a vast number of microcracks, inherent from the manufacturing process, are inevitably the source of such a delamination process. Other factors known to influence the delamination process are residual stresses due to the thermal expansion mismatches among different layers in the coating system and the presence of a thermally grown oxide layer between the top coat and the bond coat.

The present work presents a fracture mechanical analysis of the effects from thermal shock loading on inherent microcracks within the top coat close to the rough interface between the top coat and the bond coat. The analysis was performed using the finite element method, taking into account the effects of residual stresses and the presence of an oxide layer at the rough interface between top coat and bond coat. A comparative study of the risk of fracture from edge cracks compared with centrally situated cracks was performed.

Y. Liu and **C. Persson,** Division of Materials Engineering, Department of Mechanical Engineering, and **S. Melin,** Division of Solid Mechanics, Department of Mechanical Engineering, Lund University, SE-22100, Lund, Sweden. Contact e-mail: yan.liu@material.lth.se.

2. Experimental Background

Thermal shock tests of as-sprayed and pre-oxidized TBC systems have been performed at Volvo Aero Corporation (Trollhättan, Sweden) and have been reported by Liu.[1] Preheating of the substrate to a starting temperature below the steady-state mean temperature value was first performed. The substrate was thereafter subjected to cyclic temperature variations. A flame first heated the top coat side after which an air jet cooled it. The substrate backside was subjected to cooling by an air jet. The experiments showed that the most common failure mode is the spallation of the top coat by delamination, which is caused by cracks growing in the top coat close to the rough interface between the top coat and the bond coat (Fig. 1).

The test specimens consisted of a Hastelloy X substrate (6.7 mm thick and diameter 25 mm) coated with a 0.09 mm thick Ni-23Co-17Cr-12.5Al-0.5Y wt.% bond coat, which, in turn, was coated with a ceramic top coat of ZrO_2-7.5 wt.%Y_2O_3 (0.45 mm). The test specimens were pre-oxidized in an oven by holding at 1050 °C until an oxide layer of desired thickness developed between the bond coat and the top coat. The values at 700 °C for several material parameters for the different constituents are listed in Table 1.[2,3]

3. Numerical Modeling

The finite element method was used to model the experiments, employing the general-purpose finite element code ABAQUS.[4] A schematic of the model is seen in Fig. 2. The rough interface between bond coat and top coat is modeled sinusoidal with wavelength 110 μm and amplitude 12.5 μm, as estimated from measurements on the test specimens. The wavy interface expands for three wavelengths and is thereafter smoothened into a plane surface to simplify the model. An alumina oxide layer of thickness 3 μm or 6 μm is introduced above the bond coat.

For an air-plasma-sprayed TBC, the most common failure mode has been found to be the interfacial delamination in the top

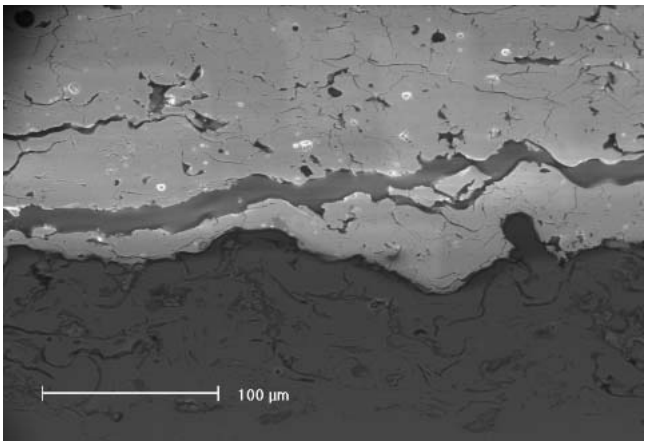

Fig. 1 Optical micrograph showing the microstructure with a delamination crack

Table 1 Material Parameters at 700°C

Layers	ZrO_2	Al_2O_3	Bond Coat	Substrate
E, GPa	17	345	103	150
Poisson's ratio	0.20	0.32	0.27	0.30
Yield stress, MPa	…	…	95	270
CTE(a), $\times 10^{-6}$/°C	11.00	7.79	15.00	15.00
Creep behavior,(b)	…	…	A = 2.04e-34	A = 3.18e-56
	…	…	B = 3.35	B = 6.00

(a) CTE, coefficient of thermal expansion
(b) Defined by the relation $\dot{\varepsilon} = A\sigma^B$, where $\dot{\varepsilon}$ is the strain rate in unit of s^{-1}, A is the creep coefficient in units of $(MPa)^{-B}\ s^{-1}$, σ is the effective von Mises stress in MPa, and B is the dimensionless creep exponent.

coat close to the oxide layer, up to 100 μm away from the interface.[1] A stationary pre-existing crack was introduced a distance d = 10 or 40 μm above an apex, parallel to the general global direction of the wavy interface. Since the stresses at the crack tip for the cracks located at d = 40 μm were found to be much lower than those for the cracks located at d = 10 μm, the cracks in the latter case are more critical and thus were investigated in this article. Depending on the boundary conditions, either a central crack of length 2a (assuming the axis A-A to be an axis of symmetry), or an edge crack of length a (the side of the cross section along the axis A-A is the free edge), is modeled, with a in the interval 5 μm < a < 180 μm.

The system was subjected to cyclic thermal loading with the temperature varying between 400 and 930 °C over a period of 300 s, and the calculations were performed in two steps, a thermal analysis followed by a mechanical analysis.

In the thermal finite element analysis, the heat flux in through the upper boundary and out of the lower boundary of the model were, for each geometric configuration, determined by an iterative procedure, resulting in a maximum discrepancy between the simulated temperatures and the experimental measurements within 2%.[1] Figure 3 shows the first few temperature cycles, with the three curves being the simulated temperatures at the TBC surface, at the substrate backside, and at the crack plane far from the crack tip. The node temperatures thus calculated were used as input for the mechanical finite element analysis.

In the mechanical finite element analysis, generalized plane

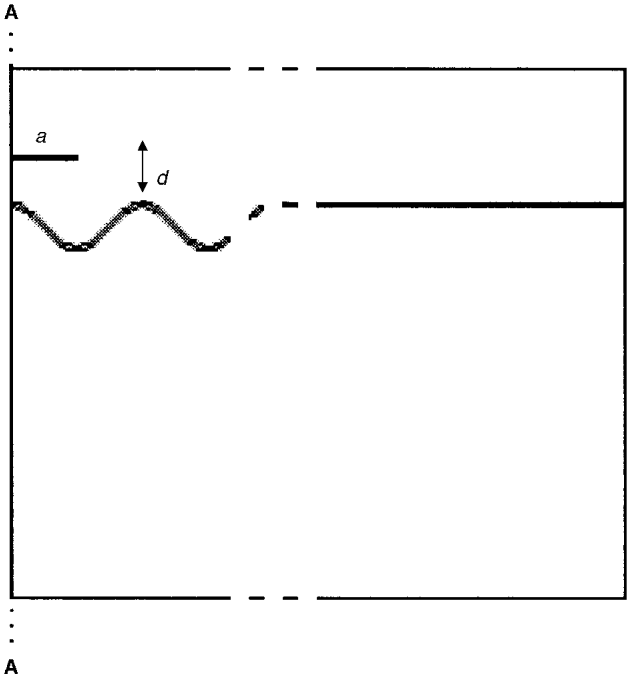

Fig. 2 Model geometry

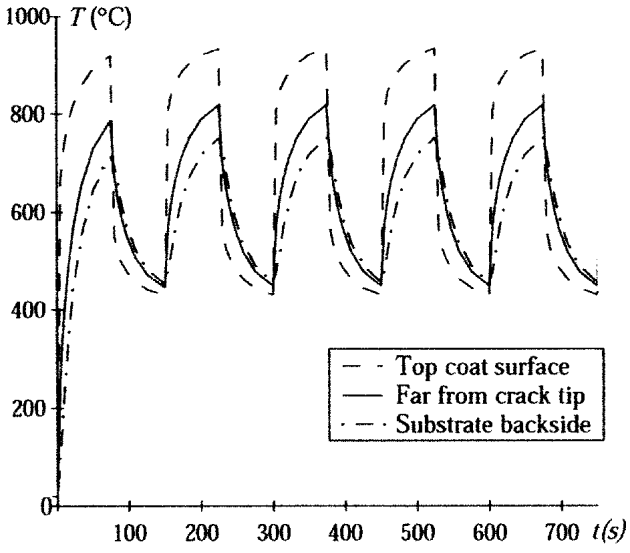

Fig. 3 Simulated temperature cycles

strain conditions were assumed, and 1071 biquadratic elements modeled the geometry. Contact elements were introduced between the crack surfaces to avoid overlap and to provide Coulomb friction between the crack surfaces whenever they were in contact. The square root singularity at the crack tip was modeled through focusing the mesh at the tip position and moving the midside nodes in the elements surrounding the tip to the quarter points.[5]

The residual stresses in the oxide layer were accounted for by imposing initial strains in the layer, which were chosen so as to induce an average hydrostatic stress of magnitude −1.4 GPa just

above an apex of the oxide layer of magnitude −1.8 GPa in a valley of the oxide layer, which is in agreement with the results of Wright et al.[6]

Temperature-dependent material parameters were used in the simulations. The bond coat and the substrate were modeled as elastic-visco plastic, following the Norton creep law and the von Mises yield criterion. The oxide layer and the top coat are modeled as linear elastic.

4. Results and Discussion

To judge the risk of fracture, mode I, K_I, and mode II, K_{II}, stress intensity factors at the crack tip were calculated continuously during the thermal cycling from the displacements at the nodes closest to the crack tip, as proposed in the study by Liu et al.[7] The simulations were pursued until steady state was reached, with steady state defined to prevail when the maximum as well as the minimum values of both K_I and K_{II} varied less than 0.1% between consecutive load cycles.

Figure 4(a) shows the maximum and minimum values of K_I at the tip of a central crack during the first load cycle (K^1_{Imax} and K^1_{Imin}, respectively) and at steady state (K^{ss}_{Imax} and K^{ss}_{Imin}, respectively), with half crack length a in the interval 5 μm < a < 180 μm. The corresponding values for K_{II} are shown in Fig. 4(b). In Fig. 5, the results for an edge crack of length a, with a in the interval 5 μm < a < 180 μm, are shown. Both Fig. 4 and 5 apply to a TBC system without the inclusion of friction between the crack surfaces.

In a brittle material, the most likely crack growth mode is mode I growth, initiating as K_I reaches the mode I fracture toughness K_{Ic}. The K_{Ic} of an air plasma sprayed TBC is in the range of 0.1~1 MPa · $m^{1/2}$.[8] As seen from a comparison of Fig. 4(a) and 5(a), the magnitudes of K_I for an edge crack exceeds that for a corresponding central crack, irrespective of crack length. This implies that an edge crack always constitutes a greater threat to the durability of the coating than does a central one.

From Fig. 5(a), it can also be concluded that, if mode I growth is initiated from an edge crack, the initiation will already have occurred during the first load cycle, since $K^1_{Imax} > K^{ss}_{Imax}$ (i.e., K_{Imax} decreases with the number of load cycles). However, K^1_{Imax} never exceeds 0.5 MPa · $m^{1/2}$, and if K_{Ic} > 0.5 MPa · $m^{1/2}$, the edge crack in the investigated interval will not propagate.

For a central crack, it is seen from Fig. 4(a) that $K^1_{Imax} > K^{ss}_{Imax}$ in the intervals of half crack length 40 μm < a < 100 μm and a > 140 μm for the crack lengths investigated in this study. Thus, for a in these intervals mode I crack initiation will take place, assuming K_{Ic} = 0.1 MPa · $m^{1/2}$, during the first load cycle, whereas it will take place at later cycles in the interval 100 μm < a < 140 μm. If K_{Ic} > 0.3 MPa · $m^{1/2}$, approximately, the mode I fracture will not occur for the investigated crack length.

It also can be seen that mode I stress intensity factors are larger for cracks with a crack tip position above a valley of the wavy interface. This applies to both edge cracks and central cracks. Thus, such cracks are more prone to propagation than are cracks with crack tip position close to an apex. Central cracks for which 110 μm < a < 130 μm, approximately, are even closed at the crack tips during the early loading cycles (i.e., $K_I \equiv 0$ in this interval).

Figures 4(b) and 5(b) show that the magnitudes of the mode II

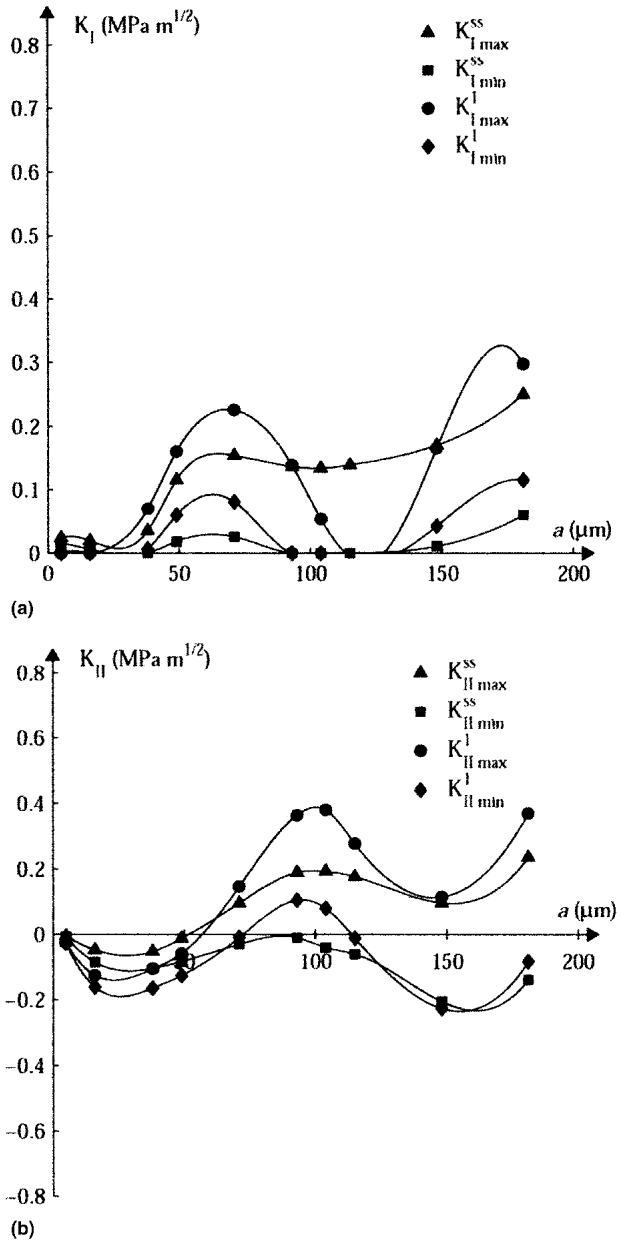

Fig. 4 Maximum and minimum values of the **(a)** mode I and **(b)** mode II stress intensity factors during the first load cycle and at steady state for centrally situated cracks. The oxide layer thickness is 3 μm.

stress intensity factors exceed the magnitudes of the mode I stress intensity factors for a given value of a, and that the magnitudes in cases of an edge crack exceed the corresponding values for a central crack. The large magnitudes of K_{II} might imply mode II fracture, even though the mode II fracture toughness K_{IIc} is much larger than K_{Ic}. In other work,[8] the ratio K_{IIc}/K_{Ic} has been estimated to be in the interval 3-5.

Even if mode I fracture is initiated, the mode II component will influence the crack propagation so as to turn the propagation direction toward perpendicular to the largest principal stress. As the crack turns, the stresses will redistribute, and to determine whether the crack will continue to propagate until the final failure of the coating, the actual crack path must be followed incre-

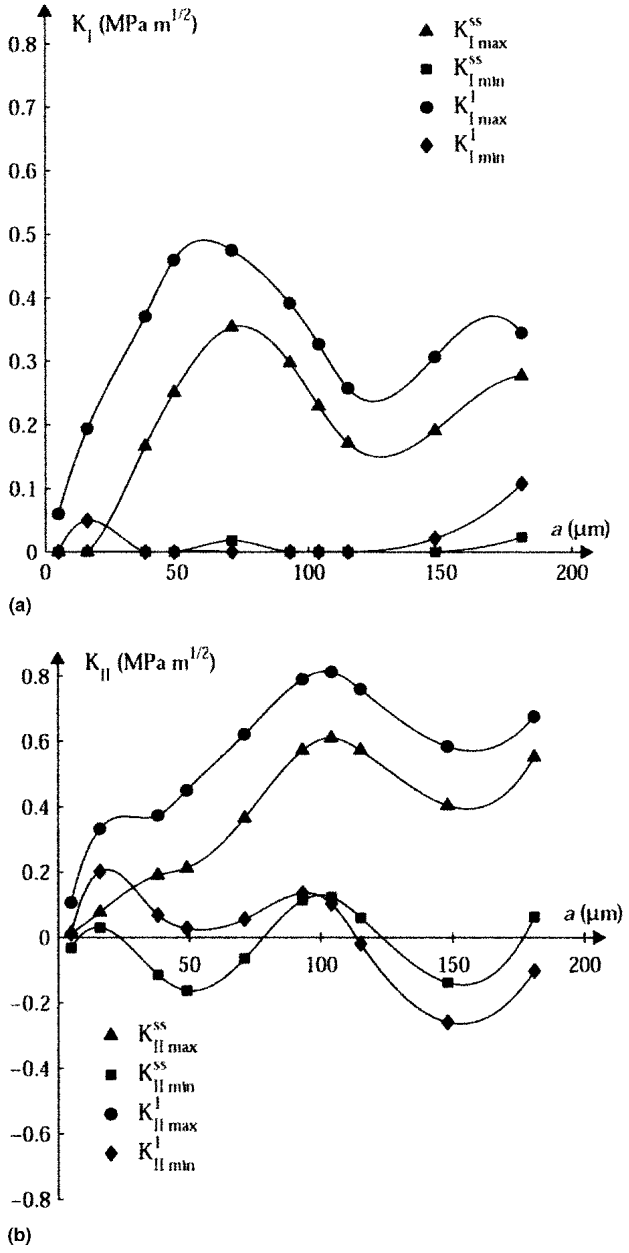

Fig. 5 Maximum and minimum values of the **(a)** mode I and **(b)** mode II stress intensity factors during the first load cycle and at steady state for edge cracks. The oxide layer thickness is 3 μm.

mentally through the loading cycles. This is, however, beyond the scope of this article.

An increase in oxide layer thickness results in an increase in the stress intensity factors for both modes I and II, and for both crack configurations. This confirms the general belief that the oxide layer weakens the TBC system.

The results that have been presented apply to calculations without friction acting between the crack surfaces if they are in contact. The inclusion of friction did not significantly alter the magnitudes of the mode I stress intensity factors. For mode II, however, the inclusion of friction decreased K_{II} as expected. Since friction always is present, this means that a mode II fracture becomes less likely than a mode I fracture.

5. Conclusions

It was found that spallation of the top coat of a TBC system due to thermal shock loading is more likely to start from an edge crack than from a centrally situated crack. It was also found that the mode I stress intensity factor at the tip of an edge crack decreases with the number of load cycles so that mode I crack growth initiation, if it occurs, has already taken place during the first load cycle.

References

1. Y. Liu: "Life Prediction and Mechanical Behaviour of Thermal Barrier Coatings," Ph.D. Thesis [ISRN LUTFD2/TFMT–03/1011– SE (1-120)], Division of Materials Engineering, Department of Mechanical Engineering, Lund University, SE–221 00, Lund, Sweden, 2003.
2. C. Persson and Y. Liu: "Life Prediction of Thermal Barrier Coatings," Final Report, Materials Engineering, Lund University, Lund, Sweden, 1998.
3. J.T. DeMasi, K.D. Sheffler, and M. Ortiz: "Thermal Barrier Coating Life Prediction Model Development," NASA Cr-182230, NASA-LeRC, Cleveland, OH, 1989.
4. ABAQUS/Standard: *ABAQUS, Version 6.3 User's Manual,* Hibbitt, Karlsson & Sorensen, Inc., Providence, RI, 2002.
5. R.S. Barsoum: "On the Use of Isoparametric Finite Elements in Linear Fracture Mechanics," *Int. J. Num. Methods Eng.,* 1976, *10,* pp. 25-37.
6. J.K. Wright, R.L. Williamson, D. Renusch, B. Veal, M. Grimsditch, P.Y. Hou, and M.R. Cannon: "Residual Stresses in Convoluted Oxide Scales," *Mater. Sci. Eng.,* 1999, *A262,* pp. 246-55.
7. Y. Liu, C. Persson, and S. Melin: "Fracture Mechanics Approach to Delamination of Thermally Cycled Thermal Barrier Coatings," in *Thermal Spray 2001: Surface Engineering via Applied Research,* C.C. Berndt, K.A. Khor, and E.F. Lugscheider, ed., ASM International, Materials Park, OH, 2001, pp. 1339-44.
8. A.G. Evans, D.R. Mumm, J.W. Hutchinson, G.H. Meier, and F.S. Pettit: "Mechanisms Controlling the Durability of Thermal Barrier Coatings," *Prog. Mater. Sci.,* 2001, *46,* pp. 505-53.